ELSEVIER

Physica A 273 (1999) 1–18

PHYSICA A

www.elsevier.com/locate/physa

Scaling features of noncoding DNA

H.E. Stanley[a,*], S.V. Buldyrev[a], A.L. Goldberger[b,d], S. Havlin[c], C.-K. Peng[a,b], M. Simons[b]

[a] *Center for Polymer Studies and Department of Physics, Boston University, Boston, MA 02215, USA*
[b] *Cardiovascular Div., Harvard Medical School, Beth Israel Hospital, Boston, MA, USA*
[c] *Department of Physics, Bar-Ilan University, Ramat-Gan, Israel*
[d] *Department of Biomedical Engineering, Boston University, Boston, MA, USA*

Received 6 September 1999

Abstract

We review evidence supporting the idea that the DNA sequence in genes containing *noncoding* regions is correlated, and that the correlation is remarkably long range — indeed, base pairs *thousands of base pairs* distant are correlated. We do not find such a long-range correlation in the coding regions of the gene, and utilize this fact to build a *Coding Sequence Finder Algorithm*, which uses statistical ideas to locate the coding regions of an unknown DNA sequence. Finally, we describe briefly some recent work adapting to DNA the Zipf approach to analyzing linguistic texts, and the Shannon approach to quantifying the "redundancy" of a linguistic text in terms of a measurable entropy function, and reporting that noncoding regions in eukaryotes display a larger redundancy than coding regions. Specifically, we consider the possibility that this result is solely a consequence of nucleotide concentration differences as first noted by Bonhoeffer and his collaborators. We find that cytosine–guanine (CG) concentration does have a strong "background" effect on redundancy. However, we find that for the purine–pyrimidine binary mapping rule, which is not affected by the difference in CG concentration, the Shannon redundancy for the set of analyzed sequences is larger for noncoding regions compared to coding regions. © 1999 Elsevier Science B.V. All rights reserved.

1. Introduction

Scaling concepts have played a key role in our understanding of phenomena occurring near critical points. A scale invariant function $f(x)$ has the remarkable property that each time x is doubled, the function $f(x)$ changes by the same factor. There is thus no way to set a characteristic scale for such a function.

* Corresponding author. Fax: +1-617-3533783.
E-mail address: hes@bu.edu (H.E. Stanley)

0378-4371/99/$ - see front matter © 1999 Elsevier Science B.V. All rights reserved.
PII: S0378-4371(99)00407-0

Stated mathematically, if the variable x is increased by an arbitrary factor λ, then the function is changed by a factor λ^p which is independent of the value of x,

$$f(\lambda x) = \lambda^p f(x) \tag{1}$$

for all λ. A functional equation, such as (1), constrains the set of possible functional forms of $f(x)$: any function $f(x)$ satisfying (1) must be a power-law, as may be seen by substituting the choice $\lambda = 1/x$ in (1),

$$f(x) = Ax^p. \tag{2}$$

We say that scale invariance [Eq. (1)] implies power-law behavior [Eq. (2)]. Conversely, power-law behavior implies scale invariance, since any function $f(x)$ obeying (2) also obeys (1) — one can verify this by substitution. Thus, scale invariance is mathematically equivalent to power-law behavior.

Power laws are found to describe various functions in the vicinity of critical points. These include not only systems with Hamiltonians (such as the Ising and Heisenberg models) but also purely geometric systems, such as percolation. Scaling is also found to hold for polymeric systems, including both linear and branched polymers. Here power-law correlations develop in the asymptotic limit in which the number of monomers approaches infinity. The list of systems in which power-law correlations appear has grown rapidly in recent years, including models of rough surfaces, turbulence, and earthquakes. In this talk, I will present recent work suggesting that — under suitable conditions — the sequence of base pairs or "nucleotides" in noncoding DNA also displays power-law correlations. The underlying basis of such power-law correlations is not understood at present, but it is at least possible that this reason is of as fundamental importance as it is in other systems in nature that have been found to display power-law correlations.

2. Information coding in DNA

Genomic sequences contain numerous "layers" of information. These include specifications for mRNA sequences responsible for protein structure, identification of coding and non-coding parts of the sequence, information necessary for specification of regulatory (promoter, enhancer) sequences, information directing protein–DNA interactions, directions for DNA packaging and unwinding. The genomic sequence is likely the most sophisticated and efficient information database created by nature through the dynamic process of evolution. Equally remarkable is the precise transformation of different layers of information (replication, decoding, etc.) that occurs in a short time interval. While means of encoding some of this information is understood (for example, the genetic code directing amino acid assembly, sequences directing intron/exon splicing, etc.), relatively little is known about other layers of information encrypted in a DNA molecule. In the genomes of high eukaryotic organisms, only a small portion of the total genome length is used for protein coding. The role of introns and intergenomic

sequences constituting a large portion of the genome remains unknown. Furthermore, only a few quantitative methods are currently available for analyzing such information.

3. Conventional statistical analysis of DNA sequences

DNA sequences have been analyzed using a variety of models that can basically be considered in two categories. The first types are "local" analyses; they take into account the fact that DNA sequences are produced in sequential order, so the neighboring base pairs will affect the next attaching base pair. This type of analysis, such as n-step Markov models, can indeed describe some observed short-range correlations in DNA sequences. The second category of analyses is more "global" in nature, concentrating on the presence of repeated patterns (such as periodic repeats and interspersed base sequence repeats) that can be found mostly in eukaryotic genomic sequences. A typical example of analysis in this category is the Fourier transform analysis which can identify repeats of certain segments of the same length in base pair sequences [1].

However, DNA sequences are more complicated than these two standard types of analysis can describe. Therefore, it is crucial to develop new tools for analysis with a view toward uncovering the mechanisms used to code other types of information in DNA sequences.

4. Scale-invariant (fractal) analysis of DNA sequences

In the last decade, scaling analysis (fractal) techniques have been developed for detecting scale-invariant statistical patterns and study physical properties in complex fluids and other random systems. These methods have been successfully applied in a number of disciplines and to a number of problems including stochastic growth processes in physics and chemistry, polymer physics, as well as other problems [2–4]. Since DNA sequences are long polymer chains, some general scale-invariant properties found in polymer physics [5,6] may appear in DNA, and alterations of those general properties may serve for characterization of DNA sequences.

A useful approach to studying stochastic properties of DNA involves the construction of a $1:1$ map of the base pair sequence projected onto a walk — which we term a "DNA walk" [7,8]. The mapping is then used to obtain a quantitative measure of the *correlation* between base pairs over long distances along the DNA chain. In addition, the technique provides a novel graphical "fingerprint" representation of DNA structures.

In this fashion we uncovered in the base pair sequence a remarkably *long-range* power-law correlation that is significant because it implies a new scale invariant (fractal) property of DNA. Such long-range correlations are limited to non-coding sequences (introns, regulatory untranscribed gene elements and intergenomic sequences) and occur in organisms as diverse as hepatitis delta agent, cytomegalovirus, yeast

chromosome and a large number of eukaryotic genes encoding a variety of proteins (see Refs. [8,9]).

The power-law decay correlations are of interest because they cannot be accounted for by the standard Markov chain model or other short-range correlations models (which will only give rise to an exponential decay in correlation). On the other hand, unlike the standard Fourier transform analysis [1] that detects the periodical repeats described by a few characteristic length scales, our analysis shows that there exist statistically self-similar patterns on all length scales.

5. The "DNA walk" or "fractal landscape" representation

In order to study the scale-invariant long-range correlations of the DNA sequences, we first introduced a graphical representation of DNA sequences, which we term a "fractal landscape" or "DNA walk". For the conventional one-dimensional random walk model, a walker moves either up $[u(i)=+1]$ or down $[u(i)=-1]$ one unit length for each step i of the walk [2]. For the case of an uncorrelated walk, the direction of each step is independent of the previous steps. For the case of a correlated random walk, the direction of each step depends on the history ("memory") of the walker. The DNA walk is defined by the rule that the walker steps up $[u(i)=+1]$ if a pyrimidine occurs at position a linear distance i along the DNA chain, while the walker steps down $[u(i)=-1]$ if a purine occurs at position i (Fig. 1)[1]. The question we asked was whether such a walk displays only short-range correlations (as in an n-step Markov chain) or long-range correlations (as in critical phenomena and other scale-free "fractal" phenomena).

The DNA walk provides a graphical representation for each gene and permits the degree of correlation in the base pair sequence to be directly visualized. This naturally motivates a quantification of this correlation by calculating the "net displacement" of

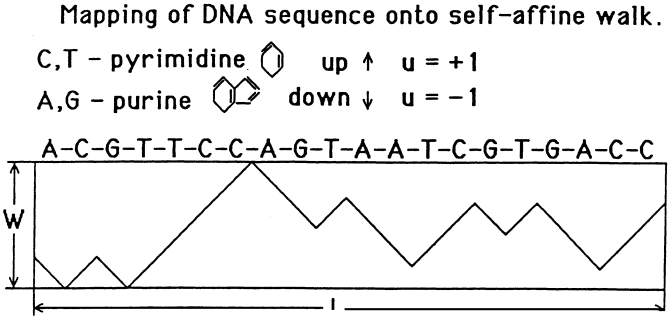

Fig. 1. Schematic illustration showing the definition of the "DNA walk".

[1] The original DNA walk proposed by Azbel [7] is based on a different rule. The walker makes a step up for a strongly bonded pair C or G and a step down for a weakly bonded pair A or T. Two-dimensional DNA walks were constructed [10] and extensively used by Cebrat et al. [11,12].

the walker after ℓ steps, which is the sum of the unit steps $u(i)$ for each step i. Thus, $y(\ell) \equiv \sum_{i=1}^{\ell} u(i)$.

An important statistical quantity characterizing any walk [2] is the root mean square fluctuation $F(l)$ about the average of the displacement; $F(\ell)$ is defined in terms of the difference between the average of the square and the square of the average,

$$F^2(\ell) \equiv \overline{[\Delta y(\ell) - \overline{\Delta y(\ell)}]^2} = \overline{[\Delta y(\ell)]^2} - \overline{\Delta y(\ell)}^2, \tag{3}$$

of a quantity $\Delta y(\ell)$ defined by $\Delta y(\ell) \equiv y(\ell_0 + \ell) - y(\ell_0)$. Here the bars indicate an *average* over all positions ℓ_0 in the gene. Operationally, this is equivalent to (a) taking a set of calipers set for a fixed distance ℓ, (b) moving the beginning point sequentially from $\ell_0 = 1$ to $\cdots$ and (c) calculating the quantity $\Delta y(\ell)$ (and its square) for each value of ℓ_0, and (d) averaging all of the calculated quantities to obtain $F^2(\ell)$. A similar function was first used to study correlations in DNA sequences by Azbel [13].

The mean square fluctuation is related to the auto-correlation function $C(\ell) \equiv \overline{u(\ell_0)/u(\ell_0 + l)} - \overline{u(\ell_0)}^2$ through the relation: $F^2(\ell) = \sum_{i=1}^{\ell} \sum_{j=1}^{\ell} C(j - i)$. The calculation of $F(\ell)$ can distinguish three possible types of behavior. (i) If the base pair sequence were random, then $C(\ell)$ would be zero on average [except $C(0) = 1$], so $F(\ell) \sim \ell^{1/2}$ (as expected for a *normal* random walk). (ii) If there were a local correlation extending up to a characteristic range R (such as in Markov chains), then $C(\ell) \sim \exp(-\ell/R)$, and for finite values of ℓ the $F(\ell)$ function would significantly deviate from $\ell^{1/2}$ [13]; nonetheless *the asymptotic behavior* $F(\ell) \sim \ell^{1/2}$ *would be unchanged from the purely random case!*. (iii) If there is no characteristic length (i.e., if the correlation were "infinite-range"), then the scaling property of $C(\ell)$ would not be exponential, but would most likely to be a power-law function, and the fluctuations will also be described by a power-law

$$F(\ell) \sim \ell^{\alpha} \tag{4}$$

with $\alpha \neq \frac{1}{2}$. In fact, the $F(\ell)$ function for real DNA sequences is not a perfect power-law, which would be true only if the log–log graph of $F(\ell)$ were a straight line. The slope of such a graph $\alpha(\ell)$ depends on ℓ. Moreover, if a DNA sequence consists of several large segments of different base pair compositions, the slope $\alpha(\ell)$ would approach 1.0 for large values of ℓ [14,15]. To take into account the DNA patchiness, the detrended fluctuation analysis (DFA) method was developed [16].

The idea of the DFA method is to compute the dependence of the standard error of a linear interpolation of a DNA walk $F_d(\ell)$ on the size of the interpolation segment ℓ. The method takes into account differences in local nucleotide content and may be applied to the entire sequence which has lengthy patches. In contrast with the original $F(\ell)$ function, which has spurious crossovers even for ℓ much smaller than a typical patch size, the detrended function $F_d(\ell)$ shows linear behavior on the log–log plot for all length scales up to the characteristic patch size, which is of the order of a thousand nucleotides in the coding sequences. For ℓ close to the characteristic patch size the log–log plot of $F_d(\ell)$ has an abrupt change in its slope.

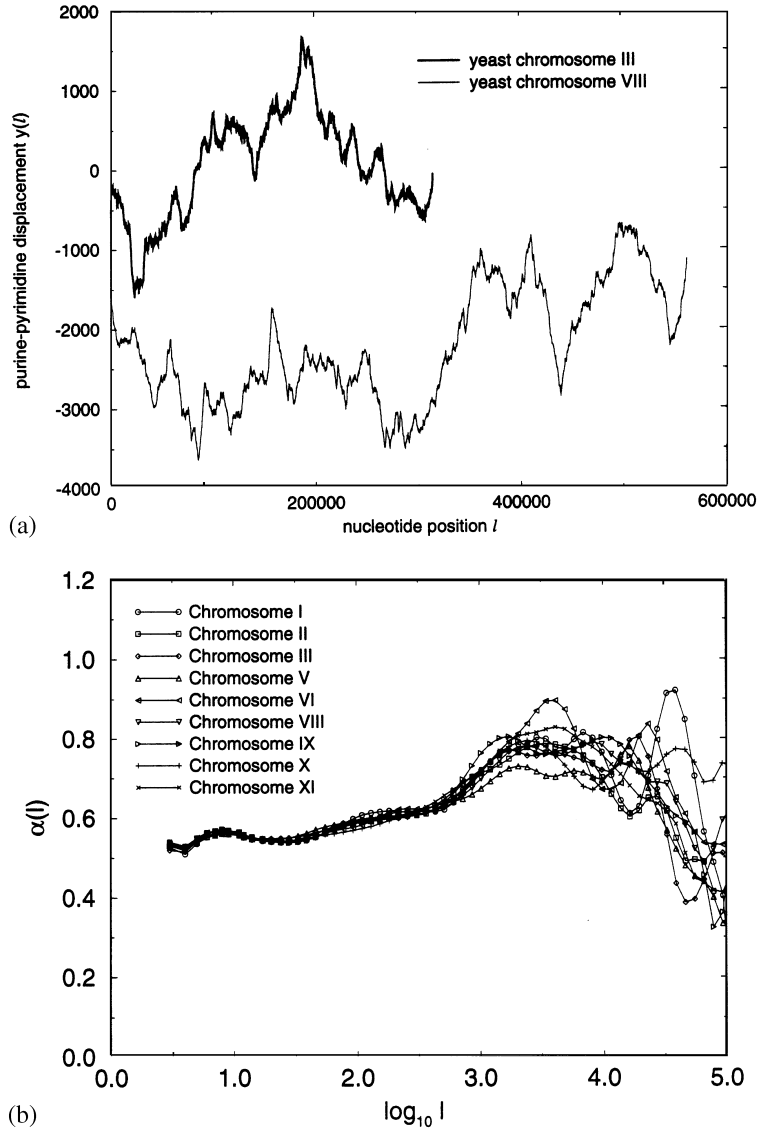

Fig. 2. (a) DNA walk for yeast chromosomes III and VIII. (b) Local exponent $\alpha(\ell)$ measured on length scale ℓ. Note that even though the 2 chromosomes have dramatically different landscapes, the $\alpha(\ell)$ functions are similar. Courtesy of Viswanathan [17].

Fig. 2 shows the DFA exponent $\alpha(\ell)$ for the nine sequenced chromosomes of *Saccharomyces cerevisiae* using the purine–pyrimidine rule and the hydrogen bond energy rule. Note that although the landscapes look quite different, the LRC exponent $\alpha(\ell)$ is very similar for different chromosomes. For $\ell < 1000$ bp the different chromosomes have almost identical $\alpha(\ell)$. This similarity indicates that the correlation properties of the different chromosomes are almost the same for $\ell < 1000$ bp. Note also how the first couple of peaks in $\alpha(\ell)$ roughly coincide for the different chromosomes in Fig. 2(b). This indicates that the nine chromosomes have similar patch sizes, because peaks in $\alpha(\ell)$ correspond to characteristic patch sizes.

The DFA method clearly supports the difference between coding and noncoding sequences, showing that the coding sequences are less correlated than noncoding

sequences for the length scales less than 1000, which is close to characteristic patch size in the coding regions. One source of this difference is the tandem repeats (sequences such as AAAAAA...), which are quite frequent in noncoding sequences and absent in the coding sequences [17].

6. Coding sequence finder (CSF) algorithm

To provide an "unbiased" test of the thesis that noncoding regions possess but coding regions lack long-range correlations, Ossadnik et al. [18] analyzed several artificial uncorrelated and correlated "control sequences" of size 10^5 nucleotides using the GRAIL neural net algorithm [19]. The GRAIL algorithm identified about 60 putative exons in the uncorrelated sequences, but only about 5 putative exons in the correlated sequences.

Using the DFA method, we can measure the local value of the correlation exponent α along the sequence (see Fig. 3) and find that the local minima of α as a function of a nucleotide position usually correspond to coding regions, while the local maxima correspond to noncoding regions. Statistical analysis using the DFA technique of the nucleotide sequence data for yeast chromosome III (315, 338 nucleotides) shows the probability that the observed correspondence between the positions of minima and coding regions is due to random coincidence is less than 0.0014. Thus, this method — which we called the "coding sequence finder" (CSF) algorithm — can be used for finding coding regions in the newly sequenced DNA, a potentially important application of DNA walk analysis.

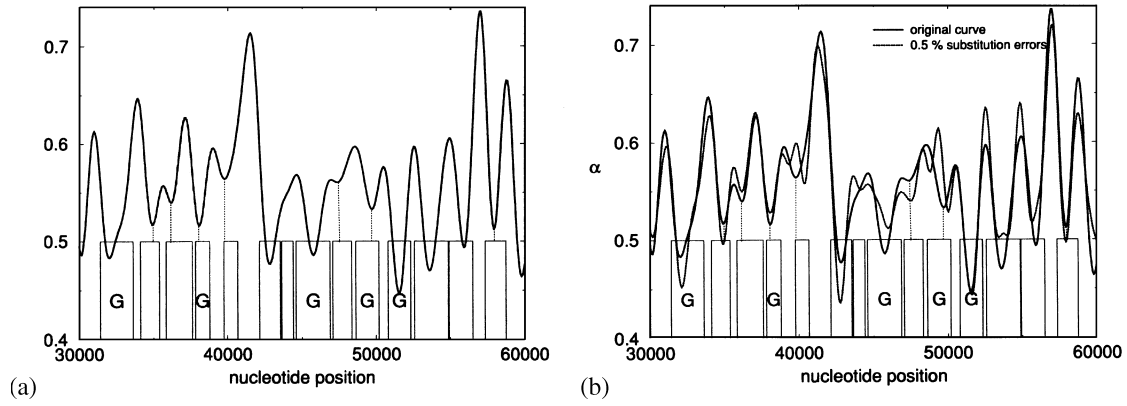

Fig. 3. (a) Analysis of section of yeast chromosome III using the sliding box *Coding Sequence Finder* "CSF" algorithm. The value of the long-range correlation exponent α is shown as a function of position along the DNA chain. In this figure, the results for about 10% of the DNA are shown (from base pair #30 000 to base pair #60 000). Shown as vertical bars are the putative genes and open reading frames; denoted by the letter "G" are those genes that have been more firmly identified (March 1993 version of *GenBank*). Note that the local value of α typically displays minima where genes are suspected, while between the genes α displays maxima. This behavior corresponds to the fact that the DNA sequences of coding regions lack power-law long range correlations ($\alpha = 0.5$ in the idealized limit), while the DNA sequences in between coding regions possess power-law long range correlations ($\alpha \approx 0.6$). Parameter values: $w = 800, \ell_1 = 8, \ell_2 = 64$. (b) The solid curve is the same as in part (a), while the dotted curve is the same analysis applied after 0.5% of the base pairs have in the same sequence been randomly mutated. With courtesy of Ossadnik [18].

7. Systematic analysis of GenBank database

An open question in computational molecular biology is whether long-range correlations are present in both coding and noncoding DNA or only in the latter. To answer this question, Buldyrev et al. [20], following the idea of Voss [21], analyzed all 33 301 coding and all 29 453 noncoding eukaryotic sequences — each of length larger than 512 base pairs (bp) — in the present release of the GenBank to determine whether there is any statistically significant distinction in their long-range correlation properties.

They found that standard fast Fourier transform (FFT) analysis indicates that *coding* sequences have practically no correlations in the range from 10 to 100 bp (spectral exponent $\beta \pm 2SD = 0.00 \pm 0.04$). Here β is defined through the relation $S(f) \sim 1/f^{\beta}$, where $S(f)$ is the Fourier transform of the correlation function, and β is related to the long-range correlation exponent α by $\beta = 2\alpha - 1$ so that $\alpha = 12$ corresponds to $\beta = 0$ (white noise).

In contrast, for *noncoding* sequences, the average value of the spectral exponent β is positive (0.16 ± 0.05), which unambiguously shows the presence of long-range correlations. They also separately analyzed the 874 coding and 1157 noncoding sequences which have more than 4096 bp, and found a larger region of power-law behavior. They calculated the probability that these two data sets (coding and noncoding) were drawn from the same distribution, and found that it is less than 10^{-10}. They also obtained independent confirmation of these findings using the DFA method, which is designed to treat sequences with statistical heterogeneity such as DNAs known mosaic structure ("patchiness") arising from non-stationarity of nucleotide concentration. The near-perfect agreement between the two independent analysis methods, FFT and DFA, increases the confidence in the reliability of the conclusion that long-range correlations exist only in noncoding sequences.

Very recently Arneodo et al. [22–25] studied long-range correlation in DLA sequences using wavelet analysis. The wavelet transform can be made blind to "patchiness" of genomic sequences. They found the existence of long-range correlations in noncoding regimes, and no long-range correlations in coding regimes in excellent agreement with Ref. [20].

8. Analysis of noncoding DNA using methods of statistical linguistics

Long-range correlations have been found also in human writings [26,27]. A novel, a piece of music or a computer program can be regarded as a one-dimensional string of symbols. These strings can be mapped to a one-dimensional random walk model similar to the DNA walk allowing calculation of the correlation exponent α. Values of α between 0.6 and 0.9 were found for various texts.

An interesting hierarchical feature of languages was found in 1949 by Zipf [28]. He observed that the frequency of words as a function of the word order ("rank")

decays as a power-law (with a power ζ close to -1) for more than four orders of magnitude.

In order to adapt the Zipf analysis to DNA, the concept of word must first be defined. In the case of coding regions, the words are the 64 3-tuples ("triplets") which code for the amino acids, AAA, AAT, ... GGG. However, for noncoding regions, the words are not known. Therefore, Mantegna et al. [29,30] consider the word length n as a free parameter, and performs analyses not only for $n = 3$ but also for all values of n in the range 3–8. The different n-tuples are obtained for the DNA sequence by shifting progressively by 1 base a window of length n; hence, for a DNA sequence containing L base pairs, we obtain $L - n + 1$ different words.

The results of the Zipf analysis for all 40 DNA sequences analyzed are summarized in Ref. [29]. The averages for each category support the observation that ζ is consistently larger for the noncoding sequences, suggesting that the noncoding sequences have features more similar to a natural language than the coding sequences. Moreover, the frequency of "words" used in coding and noncoding sequences appear in quite different orders (Fig. 4).

Related interesting statistical measures of short-range correlations in languages are the entropy and redundancy. The redundancy is a manifestation of the *flexibility* of the underlying code. To quantitatively characterize the redundancy implicit in the DNA sequence, we utilize the approach of Shannon, who provided a mathematically precise definition of redundancy [31,32].

Mantegna et al. [29] applied Shannon n-tuple redundancy analysis to study long DNA sequences. Analyzing GenBank sequences of eukaryotic and viral DNA of length more than 50 000 bp, as well as three entire chromosomal sequences, Mantegna et al. found a greater redundancy of noncoding compared to coding regions in the majority of the cases studied. Here we discuss the possibility — first raised by Bonhoeffer et al. [33] — that the observed increase in redundancy for noncoding regions compared to coding regions may be related to the differences in nucleotide compositions between coding and noncoding sequences.

The Shannon n-tuple redundancy for a symbolic sequence composed by 4 symbols (such as A, C, G and T in DNA) is defined to be

$$R_n \equiv 1 + \frac{1}{2n} \sum_{i=1}^{4^n} P_i \log_2 P_i, \tag{5}$$

where P_i $(1 \leqslant i \leqslant 4^n)$ is the probability of finding a certain n-tuple (see e.g. [29] and references cited therein). For completely uncorrelated sequences with equal nucleotide concentration, $P_i = 1/4^n$, so $R_n = 0$. In the opposite extreme case in which only one nucleotide is used, $R_n = 1$. Note that if $P_i = 0$, we set $P_i \log_2 P_i \equiv 0$.

It is known [34,35] that the usage of strongly bonded nucleotide C–G pairs is usually less frequent than the usage of weakly bonded A–T (adenine–thymine) pairs. Furthermore, the C–G concentration may differ significantly between organisms, but is generally larger in coding than in noncoding regions. The biological meaning of the existing difference between C–G vs. A–T usage in DNA sequences is not completely

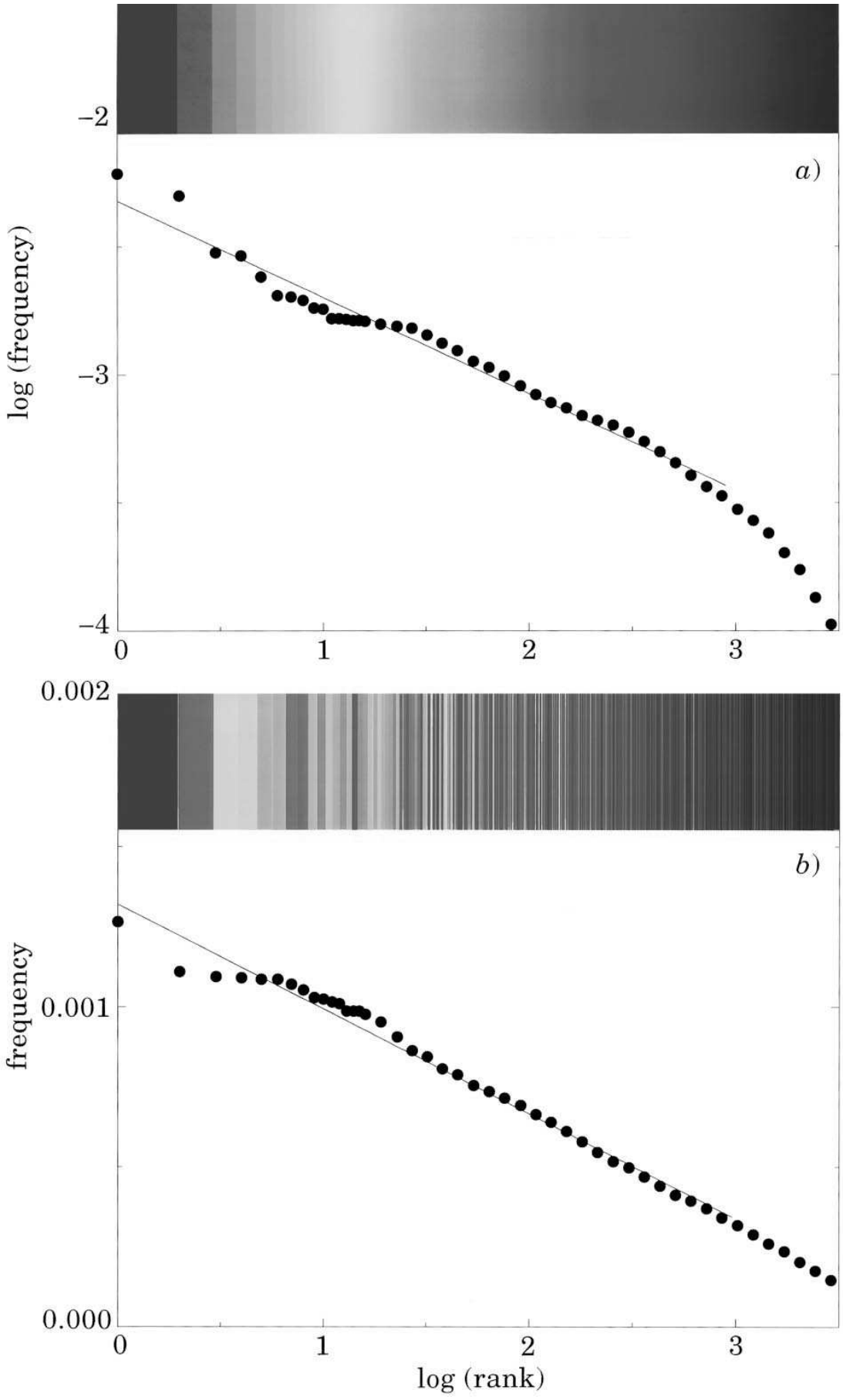
a)
log (frequency)
−2
−3
−4
0
1
2
3
b)
frequency
0.002
0.001
0.000
0
1
2
3
log (rank)

understood at the present stage. It is possible that it is related to the mechanism of DNA duplication during cell division [36,37].

Let us denote $p(C)$, $p(G)$, $p(A)$ and $p(T)$, the fractional occurrence of each nucleotide. We calculate the n-tuple redundancy of a DNA sequence using the simplest assumptions of random uncorrelated distribution of nucleotides in the sequences with $p(C)=p(G)=[p(C)+p(G)]/2=x/2$ and $p(A)=p(T)=[p(A)+p(T)]/2=(1-x)/2$.

The probability of certain n-tuple, P_i, therefore, is

$$P_i = \frac{x^k(1-x)^{n-k}}{2^n}, \tag{6}$$

where k is the number of $C+G$ in this n-tuple. The total number of such n-tuples is $C_n^k 2^n$, where 2^n comes from the fact that one can substitute a base pair by its complement without changing k.

Thus, the n-tuple redundancy $R_n(x)$ for a given concentration x of C+G is

$$R_n(x) = 1 + \frac{1}{2n}\sum_{k=0}^{n} C_n^k x^k (1-x)^{n-k}\left[k\log_2 x + (n-k)\log_2(1-x) - n\right]. \tag{7}$$

Since $\sum_{k=0}^{n} C_n^k y^k z^{n-k} k = y(\partial/\partial y)(y+z)^n = yn(y+z)^{n-1}$, it follows that,

$$R_n(x) = \tfrac{1}{2} + \tfrac{1}{2}x\log_2 x + \tfrac{1}{2}(1-x)\log_2(1-x). \tag{8}$$

Thus, $R_n(x)$ is independent of n and has a minimum value of 0 when $x=\frac{1}{2}$ also a maximum value of $\frac{1}{2}$ when $x=0$ or 1. For real DNA sequences, correlations exist between base pairs. These correlations lead to an increase of n-tuple redundancy (less random) with n. Thus, for real DNA sequences, Eq. (8) can be regarded only as the first-order approximation.

Eq. (8) shows that the n-tuple redundancy strongly depends on the CG content. To examine the effect of CG concentration on R_n for actual coding and noncoding DNA sequences, we apply the following procedure:

(1) Divide the sequence into coding and noncoding subsequences using the information from the GenBank database.

(2) Divide each coding and noncoding region into non-overlapping windows of $N=$ 500 bp. Count the numbers of G and C, N_C+N_G, in this window. Compute the CG

←

Fig. 4. Linguistic features of noncoding DNA. (a) Log–log plot of a histogram of word frequency for the noncoding part of Yeast Chromosome III (≈315 000 bp). The 6-character words are placed in rank order, where rank 1 corresponds to the most frequently used word, rank 2 to the second most frequently used word, and so forth. The straight line behavior provides evidence for a structured language in noncoding DNA. Rainbow color code corresponds to the rank of words in the language of this sequence, which is used as a "reference language" below. (b) Linear-log plot of word frequency histogram for the *coding* part of the same chromosome. The straight line behavior shows that the coding part lacks the statistical properties of a structured language. The colors are re-arranged, corresponding to the re-arrangements of their rank with respect to the reference language.

concentration of this window $x = (N_C + N_G)/N$. Select the interval of CG concentrations $[x_K - \delta x, x_K + \delta x]$, which contains the obtained value x (we choose $x_K = 0.05K$, $K = 0, 1, 2, \ldots, 20$, and $\delta x = 0.025$). Add this window to the Kth "bin" of the *CG* concentration.

(3) Count the n-tuple occurrences for $n = 1, 2, 3, 4$ in each *CG* concentration bin for coding and noncoding subsequences separately (n-tuples were counted as overlapping, n-base-pair subsequences starting at any position in the sequence). Due to the finite length of the present available DNA sequences, we are limited to low values of n to ensure the convergence of the measurements — implying a severe limitation in the investigation of higher-order Markovian (or non-Markovian) processes.

(4) Using the definition of the n-tuple redundancy in Eq. (5), compute $R_n(x)$ for each bin of the CG concentration.

Fig. 5a represents the behavior of $R_4(x)$ vs. x for coding and noncoding subsequences of four complete chromosomes of yeast (III, VI, IX, and XI). We note that $R_1(x)$ (not shown in Fig. 5a) practically coincides with the theoretical estimation (shown by a continuous line) of Eq. (8). This indicates that concentrations $p(A) \approx p(T)$ and $p(C) \approx p(G)$ for both coding and noncoding subsequences. For $n > 1$, the values of $R_n(x)$ are significantly larger than the prediction of Eq. (8), indicating the presence of correlations between nucleotides. Note that the values of $R_n(x)$ for coding and noncoding subsequences display very small differences (Fig. 5). However, the histogram of number of windows with different *CG* concentration is quite different for coding and noncoding subsequences (see Fig. 5b). For example, for yeast, the maximum of the distribution of coding is at $x_c \approx 0.4$, while for noncoding it is $x_{nc} \approx 0.35$. These maxima make the main contribution to the overall n-tuple redundancy (computed without separating different CG concentration regions). Since $R_n(x_c) < R_n(x_{nc})$, the overall n-tuple redundancy for coding DNA is expected to be lower than for noncoding DNA (see Fig. 5c). This is consistent with previous results [29]. Similarly, the CG concentration has a strong effect for most other sequences from the GenBank. We have separately analyzed groups of sequences belonging to the categories of plants, invertebrates, and vertebrates.

Of particular interest are the long primate sequences (larger than 20 000 bp) presented in Fig. 6. Note that for primate sequences $x_c \approx 0.6$, while $x_{nc} \approx 0.4$ (see Fig. 6b), which have roughly the same value of $R_n(x)$, since now x_c and x_{nc} are symmetrically located on different sides of the minima of $R_n(x)$. That may explain why the overall n-tuple redundancy for coding and noncoding subsequences in primates is practically indistinguishable (see Fig. 6c). The general term "noncoding DNA" means intergenic for yeast and intronic DNA for primates (the results for intergenic subsequences for primates are roughly intermediate between the results obtained for introns and those for coding DNA). The data for several groups of vertebrates present in the GenBank are similar to those for primates, while the data for *C. elegans* are similar to that of yeast.

These findings indicate that the non-uniform nucleotide base concentration has a significant effect on the n-tuple Shannon redundancy. Therefore, at first glance one

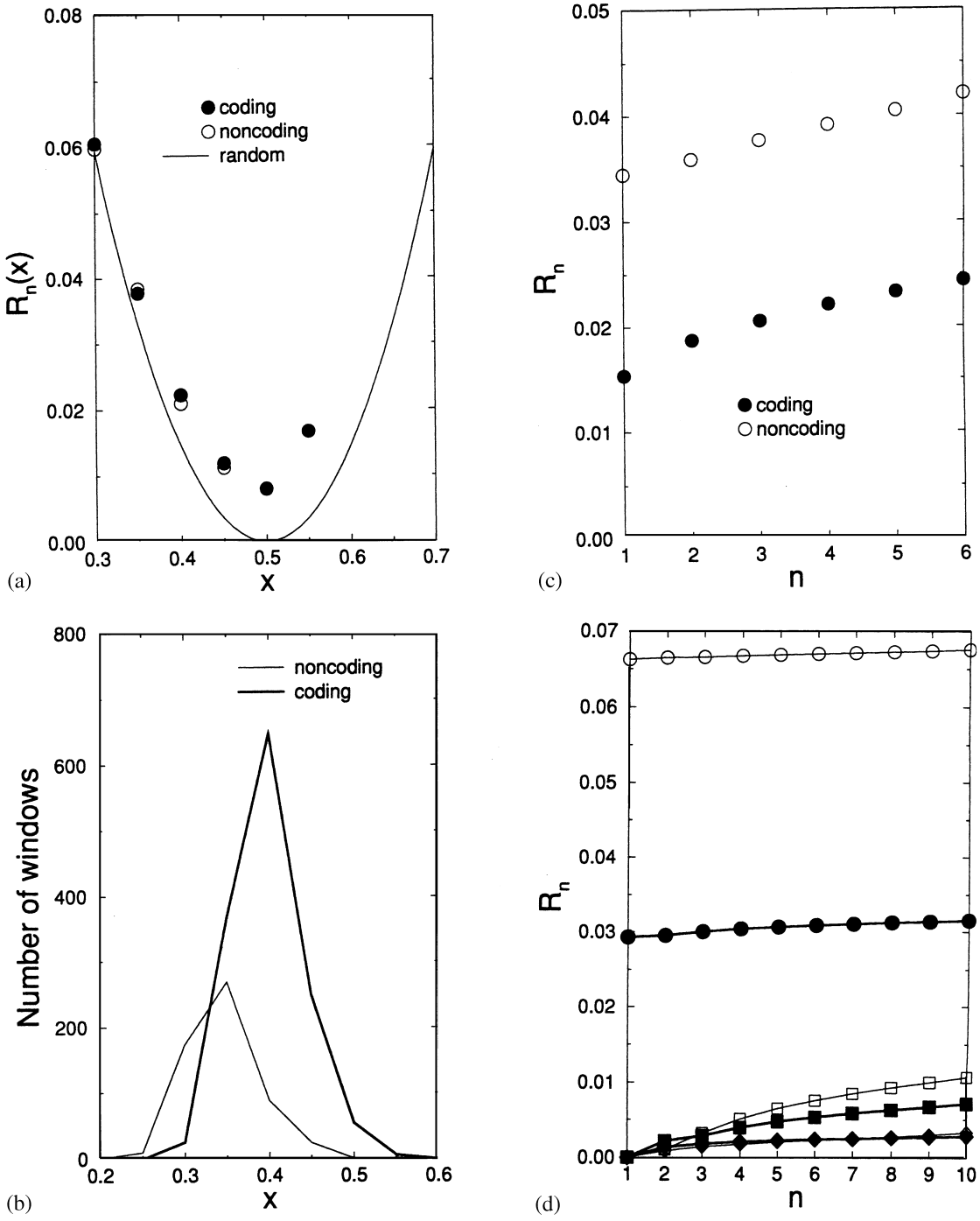

Fig. 5. (a) The n-tuple redundancy $R_4(x)$ for (●) coding and (○) noncoding subsequences in yeast chromosomes III, VI, IX, and XI. In this paper, we consistently show all the data for which sufficient statistics exist — specifically for each DNA sequence of length L, we report the redundancy R_n for values of n fulfilling the condition $L > 100 \times 4^n$ [29]. The solid line gives the predictions for the control, Eq. (8). (b) The distribution of total subsequence lengths (number of windows of size > 500 bp) with given CG concentration for coding regions (solid line) and noncoding regions (dashed line). (c) The overall n-tuple redundancy R_n vs. n for the 4-letter code. (d) Results of R_n vs. n for three different binary rules: R/Y (squares), K/M (diamonds), and S/W (circles).

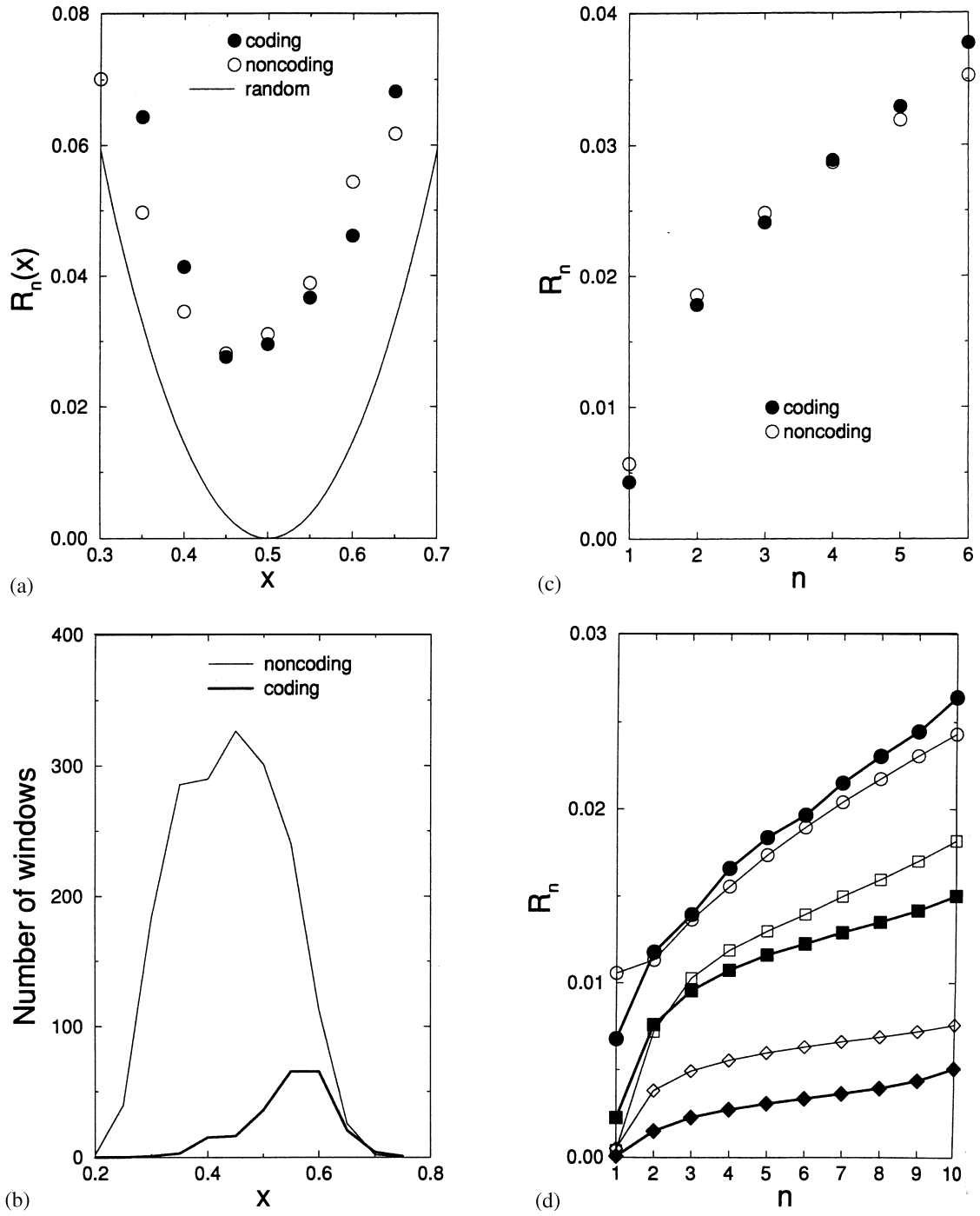

Fig. 6. The same as Fig. 5 for all primate DNA sequences longer than 20 000 bp.

might be tempted to hypothesize that the difference of n-tuple redundancy observed in coding and noncoding subsequences could be a manifestation of the overall difference of C–G concentration between coding and noncoding subsequences. On the other hand, the n-tuple redundancy measure, although robust, is not an extremely sensitive tool when a bias in the use of a subset of symbolic letters is present.

To systematically examine whether the differences in R_n between coding and noncoding regions are *completely* due to variations in CG content, we need to study the n-tuple redundancy after the effect of different concentration is removed. In order to do this, we map the 4 symbols onto a binary code in which C is one element and G the other. There are two such binary rules: (i) the R/Y rule, where R denotes a purine (A or G), and Y denotes a pyrimidine (C or T), and (ii) the K/M rule, where K denotes G or T and M denotes A or C. As a "control", we also carry out parallel studies of the third binary rule that do not distinguish C and G, (iii), the S/W rule, where S ("strong") denotes C or G, and W ("weak") denotes A or T.

We first demonstrated that while the C and G concentrations of coding and noncoding are quite different, the R and Y concentrations are almost identical — as are the concentrations of K and M. Our results for the function R_n using each of the 3 rules are shown for representative systems, yeast in Fig. 5d and primates in Fig. 6d.

Perhaps not surprisingly, the S/W rule leads to similar results as the 4-letter rule (shown in Fig. 5c), thus confirming that CG concentration makes a strong "background" contribution to any possible differences between noncoding and coding subsequences. *However, for the R/Y rule, Figs. 5d and 6d show that, the noncoding subsequences have larger redundancy than the coding subsequences.* Note that these differences are much smaller than the differences generated by CG concentration effect, so will not be visible in 4-symbol analysis. The difference in redundancy of coding and noncoding DNA for the RY rule may be related to the abundance of repeats in noncoding sequences (relative to coding) [38].

In summary, we have seen that nucleotide concentration differences may play a major role in the n-tuple redundancy statistics, so more sophisticated analysis methods that take into account this concentration effect are required. When we map the DNA sequences to binary symbolic sequences according to the R/Y rule that is independent of C–G concentration, the dominant "background" effect of CG concentration is eliminated. Moreover, we still observe higher n-tuple redundancy for noncoding subsequences. This higher redundancy cannot be simply attributed to the concentration effect.

9. Outlook for the future

There is a mounting body of evidence suggesting that the noncoding regions of DNA are rather special for at least two reasons:

(1) They display long-range power-law correlations, as opposed to previously believed exponentially decaying correlations.

(2) They display features common to hierarchically structured languages — specifically, a linear Zipf plot and a non-zero redundancy.

These results are consistent with the possibility that the noncoding regions of DNA are not merely "junk" but rather have a purpose. What that purpose could be is the subject of ongoing investigation. In particular, the apparent increase of α with evolution [39] could provide insight.

In the event that the purpose is not profound, our results nonetheless may have important practical value since quantifiable differences between coding and noncoding regions of DNA can be used to help distinguish the coding regions [18]. The results of the systematic and inclusive analysis of GenBank DNA sequences are notable for two major reasons.

(i) The GenBank data unambiguously demonstrate that noncoding DNA, but not coding DNA, possesses long-range correlations. This finding is made using two independent, complementary techniques: Fourier analysis and DFA, a modification of root-mean-square analysis of random walks. Indeed, as shown in Tables I and II of Ref. [20], the spectral exponent β computed by both techniques for the same sequence, is nearly identical.

(ii) The GenBank data demonstrate an increase in the complexity of the noncoding DNA sequences with evolution. The value of β for vertebrates is significantly greater than that for invertebrates. This finding based on the full GenBank data set supports the suggestion based upon a systematic study of the myosin heavy gene family that there is an apparent increase in the complexity of noncoding DNA for more highly evolved species compared to less evolved ones [39].

The ultimate meaning of long-range correlations is still not clear. It is possible that they are related to the spatial configuration of DNA [40]. It is also possible that long-range correlations exist also in other systems of biological interest. For example, the idea of long-range correlations has been extended to the analysis of the beat-to-beat intervals in the normal and diseased heart [41–44], to weather [45], and to human gait [46]. The healthy heartbeat is generally thought to be regulated according to the classical principle of homeostasis whereby physiologic systems operate to reduce variability and achieve an equilibrium-like state [47]. We find, however, that under normal conditions, beat-to-beat fluctuations in heart rate display the kind of long-range correlations typically exhibited by physical dynamical systems far from equilibrium, such as those near a critical point. Specifically, we find evidence for such power-law correlations that extend over thousands of heartbeats in healthy subjects. In contrast, heart rate time series from patients with severe congestive heart failure show a breakdown of this long-range correlation behavior, with the emergence of a characteristic short-range time scale. Similar alterations in correlation behavior may be important in modeling the transition from health to disease in a wide variety of pathologic conditions [48–50].

Acknowledgements

We are grateful to many individuals, including R.N. Mantegna, M.E. Matsa, S.M. Ossadnik, and F. Sciortino, for major contributions to those results reviewed here that represent collaborative research efforts. We also wish to thank C. Cantor, C. DeLisi, M. Frank-Kamenetskii, A.Yu. Grosberg, G. Huber, I. Labat, L. Liebovitch, G.S. Michaels, P. Munson, R. Nossal, R. Nussinov, R.D. Rosenberg, J.J. Schwartz, M. Schwartz,

E.I. Shakhnovich, M.F. Shlesinger, N. Shworak, and E.N. Trifonov for valuable discussions. Partial support was provided by the National Science Foundation, National Institutes of Health (Center for Biomedical Signals and Human Genome Project), the G. Harold and Leila Y. Mathers Charitable Foundation, the National Heart, Lung and Blood Institute, the National Aeronautics and Space Administration, the Israel-USA Binational Science Foundation, Israel Academy of Sciences, and (to C-KP) by an NIH/NIMH Postdoctoral NRSA Fellowship.

References

[1] S. Tavaré, B.W. Giddings, in: M.S. Waterman (Ed.), Mathematical Methods for DNA Sequences, CRC Press, Boca Raton, FL, 1989, pp. 117–132, and refs. therein.
[2] E.W. Montroll, M.F. Shlesinger, in: J.L. Lebowitz, E.W. Montroll (Eds.), Nonequilibrium Phenomena II. From Stochastics to Hydrodynamics, North-Holland, Amsterdam, 1984, pp. 1–121.
[3] H.E. Stanley, N. Ostrowsky (Eds.), On Growth and Form: Fractal and Non-Fractal Pattern in Physics, Martinus Nijhoff Publishers, Dordrecht, 1986.
[4] A. Bunde, S. Havlin (Eds.), Fractals and Disordered Systems, Springer, Berlin, 1991.
[5] P.G. de Gennes, Scaling Concepts in Polymer Physics, Cornell University Press, Ithaca NY, 1979.
[6] J. des Cloiseaux, J. Phys. (Paris) 41 (1980) 223.
[7] M.Y. Azbel, Phys. Rev. Lett. 31 (1973) 589.
[8] C.-K. Peng, S.V. Buldyrev, A.L. Goldberger, S. Havlin, F. Sciortino, M. Simons, H.E. Stanley, Nature 356 (1992) 168.
[9] W. Li, K. Kaneko, Europhys. Lett. 17 (1992) 655.
[10] C.L. Berthelsen, J.A. Glazier, M.H. Skolnick, Phys. Rev. A 45 (1992) 8902.
[11] S. Cebrat, M.R. Dudek, Eur. Phys. J. B 3 and 117 (1998) 271, 78.
[12] S. Cebrat, M.R. Dudek, A. Gierlik, M. Kowalczuk, P. Mackiewicz, Physica A 265 (1999) 78.
[13] M.Y. Azbel, Biopolymers 21 (1982) 1687.
[14] M.Y. Azbel, Phys. Rev. Lett. 75 (1995) 168.
[15] S. Karlin, V. Brendel, Science 259 (1993) 677.
[16] C.-K. Peng, S.V. Buldyrev, S. Havlin, M. Simons, H.E. Stanley, A.L. Goldberger, Phys. Rev. E 49 (1994) 1685.
[17] G.M. Viswanathan, S.V. Buldyrev, S. Havlin, H.E. Stanley, Biophys. J. 72 (1997) 866.
[18] S.M. Ossadnik, S.V. Buldyrev, A.L. Goldberger, S. Havlin, R.N. Mantegna, C.-K. Peng, M. Simons, H.E. Stanley, Biophys. J. 67 (1994) 64.
[19] E.C. Uberbacher, R.J. Mural, Proc. Nat. Acad. Sci. USA 88 (1991) 11 261.
[20] S.V. Buldyrev, A.L. Goldberger, S. Havlin, R.N. Mantegna, M.E. Matsa, C.-K. Peng, M. Simons, H.E. Stanley, Phys. Rev. E 51 (1995) 5084.
[21] R. Voss, Phys. Rev. Lett. 68 (1992) 3805.
[22] A. Arneodo, E. Bacry, P.V. Graves, J.F. Mugy, Phys. Rev. Lett. 74 (1995) 3293.
[23] A. Arneodo, Y. d'Aubenton-Carafa, E. Bacry, P.V. Graves, J.F. Muzy, C. Thermes, Physica D 96 (1996) 291.
[24] A. Arneodo, Y. d'Aubenton-Carafa, B. Audit, E. Bacry, J.F. Muzy, C. Thermes, Eur. Phys. J. B 1 (1998) 259.
[25] A. Arneodo, Y. d'Aubenton-Carafa, B. Audit, E. Bacry, J F. Muzy, C. Thermes, Physica A 249 (1998) 439.
[26] A. Schenkel, J. Zhang, Y-C. Zhang, Fractals 1 (1993) 47.
[27] M. Amit, Y. Shmerler, E. Eisenberg, M. Abraham, N. Shnerb, Fractals 2 (1994) 7.
[28] G. K. Zipf, Human Behavior and the Principle of "Least Effort", Addison-Wesley, New York, 1949.
[29] R.N. Mantegna, S.V. Buldyrev, A.L. Goldberger, S. Havlin, C.-K. Peng, M. Simons, H.E. Stanley, Phys. Rev. Lett. 73 (1994) 3169.
[30] R.N. Mantegna, S.V. Buldyrev, A.L. Goldberger, S. Havlin, C.-K. Peng, M. Simons, H.E. Stanley, Phys. Rev. E 52 (1995) 2939.

[31] L. Brillouin, Science and Information Theory, Academic Press, New York, 1956.
[32] C.E. Shannon, Bell Systems Technol. J. 80 (1951) 50.
[33] S. Bonhoeffer, A.V.M. Herz, M.C. Boerlijst, S. Nee, M.A. Nowak, R.M. May, Phys. Rev. Lett. 76 (1996) 1977.
[34] J.D. Watson, M. Gilman, J. Witkowski, M. Zoller, Recombinant DNA, Scientific American Books, New York, 1992.
[35] W.-H. Li, D. Graur, Fundamentals of Molecular Evolution, Sinauer Associates, Sunderland MA, 1991.
[36] X. Gu, W.-H. Li, J. Mol. Evol. 38 (1994) 468.
[37] S.V. Buldyrev, N.V. Dokholyan, A.L. Goldberger, S. Havlin, C.-K. Peng, H.E. Stanley, G.M. Viswanathan, Physica A 249 (1998) 430.
[38] S.V. Buldyrev et al., Physica A 273 (1999) 19–32 [these proceedings].
[39] S.V. Buldyrev, A.L. Goldberger, S. Havlin, C.-K. Peng, H.E. Stanley, M.H.R. Stanley, M. Simons, Biophys. J. 65 (1993) 2673.
[40] A.Yu. Grosberg, Y. Rabin, S. Havlin, A. Neer, Europhys. Lett. 23 (1993) 373.
[41] C.-K. Peng, J. Mietus, J. Hausdorff, S. Havlin, H.E. Stanley, A.L. Goldberger, Phys. Rev. Lett. 70 (1993) 1343.
[42] C.-K. Peng, S. V. Buldyrev, J.M. Hausdorff, S. Havlin, J.E. Mietus, M. Simons, H.E. Stanley, A.L. Goldberger, in: G.A. Losa, T.F. Nonnenmacher, E.R. Weibel (Eds.), Fractals in Biology and Medicine, Birkhauser Verlag, Boston, 1994.
[43] C.K. Peng, S. Havlin, H.E. Stanley, A.L. Goldberger, Chaos 5 (1995) 82.
[44] C. K. Peng, J.M. Hausdorff, J.E. Mietus, S. Havlin, H.E. Stanley, A.L. Goldberger, in: U. Frisch, M.F. Shlesinger, G. Zaslavsky (Eds.), Proceedings of the 1993 International Conference on Lévy Flights, Springer, Berlin, 1995.
[45] E. Koscielny-Bunde, A. Bunde, S. Havlin, H.E. Roman, Y. Goldreich, H.-J. Schellnhuber, Phys. Rev. Lett. 81 (1998) 729.
[46] J.M. Hausdorff, C.-K. Peng, Z. Ladin. J.Y. Wei, A.L. Goldberger, J. Appl. Physiol. 78 (1995) 349.
[47] W.B. Cannon, Physiol. Rev. 9 (1929) 399.
[48] P.Ch. Ivanov, M.G. Rosenblum, C.-K. Peng, J. Mietus, S. Havlin, H.E. Stanley, A.L. Goldberger, Nature 383 (1996) 323.
[49] P.Ch. Ivanov, L.A.N. Amaral, A.L. Goldberger, H.E. Stanley, Europhys. Lett. 43 (1998) 363.
[50] P.Ch. Ivanov, L.A.N. Amaral, A.L. Goldberger, S. Havlin, M.G. Rosenblum, Z. Struzik, H.E. Stanley, Nature 399 (1999) 461.